HHS Public Access

Author manuscript

Neuropathol Appl Neurobiol. Author manuscript; available in PMC 2021 October 01.

Published in final edited form as:

Neuropathol Appl Neurobiol. 2020 October ; 46(6): 546–563. doi:10.1111/nan.12596.

CHRONIC ACTIVATION OF ANTIOXIDANT PATHWAYS AND IRON ACCUMULATION IN EPILEPTOGENIC MALFORMATIONS

Till S. Zimmer[1], **Giulia Ciriminna**[1], **Andrea Arena**[1,2], **Jasper J. Anink**[1], **Anatoly Korotkov**[1], **Floor E. Jansen**[3], **Wim van Hecke**[4], **Wim G. Spliet**[4], **Peter C. van Rijen**[5], **Johannes C. Baayen**[6], **Sander Idema**[6], **Nicholas R. Rensing**[7], **Michael Wong**[7], **James D. Mills**[1], **Erwin A. van Vliet**[1,8,*], **Eleonora Aronica**[1,9,*]

[1]Amsterdam UMC, University of Amsterdam, Department of (Neuro)Pathology, Amsterdam Neuroscience, Amsterdam, the Netherlands [2]Sapienza University of Rome, Department of Biochemical Sciences, Rome, Italy [3]University Medical Center Utrecht, Department of Paediatric Neurology, Utrecht, the Netherlands [4]University Medical Center Utrecht, Department of Pathology, Utrecht, the Netherlands [5]University Medical Center Utrecht, Brain Centre, Rudolf Magnus Institute for Neuroscience, Department of Neurosurgery, Utrecht, the Netherlands [6]Amsterdam UMC, Vrije Universiteit Amsterdam, Department of Neurosurgery, Amsterdam Neuroscience, Amsterdam, the Netherlands [7]Washington University, Department of Neurology, Saint Louis, MO, United States of America [8]University of Amsterdam, Swammerdam Institute for Life Sciences, Center for Neuroscience, Amsterdam, the Netherlands [9]Stichting Epilepsie Instellingen Nederland (SEIN), Heemstede, the Netherlands

Abstract

Aims: Oxidative stress is evident in resected epileptogenic brain tissue of patients with developmental brain malformations related to mammalian target of rapamycin activation: tuberous sclerosis complex (TSC) and focal cortical dysplasia type IIb (FCD IIb). Whether chronic activation of anti-oxidant pathways is beneficial or contributes to pathology is not clear.

Methods: We investigated oxidative stress markers, including haem oxygenase 1, ferritin and the inflammation associated microRNA-155 in surgically resected epileptogenic brain tissue of TSC (n = 10) and FCD IIb (n = 8) patients and in a TSC model (*Tsc1*$^{GFAP-/-}$ mice) using immunohistochemistry, *in situ* hybridization, real-time quantitative PCR, and immunoblotting. Using human fetal astrocytes we performed an *in vitro* characterization of the anti-oxidant

Corresponding author: Dr. E. Aronica, Amsterdam UMC, University of Amsterdam, Dept. (Neuro)Pathology, Meibergdreef 9, 1105 AZ, Amsterdam, the Netherlands, Phone: + 31 20 5664369, e.aronica@amsterdamumc.nl.

*these authors are joint senior author

Competing interests

The authors declare that they have no conflict of interest.

Ethical approval

All procedures performed in studies involving human participants were in accordance with the Amsterdam UMC Research Code provided by the Medical Ethics Committee and with the 1964 Helsinki declaration and its later amendments or comparable ethical standards. All procedures performed in studies involving animals were in accordance with the ethical standards of the Washington University Animal Welfare committee.

response to acute and chronic oxidative stress and evaluated overexpression of the disease relevant pro-inflammatory microRNA-155

Results: Resected TSC or FCD IIb tissue displayed higher expression of oxidative stress markers and microRNA-155. *Tsc1*$^{GFAP-/-}$ mice expressed more microRNA-155 and haem oxygenase 1 in the brain compared to wild type, preceding the typical development of spontaneous seizures in these animals. *In vitro*, chronic microRNA-155 overexpression induced haem oxygenase 1, iron regulatory elements and increased susceptibility to oxidative stress. Overexpression of iron regulatory genes was also detected in patients with TSC, FCD IIb and *Tsc1*$^{GFAP-/-}$ mice.

Conclusion: Our results demonstrate that early and sustained activation of anti-oxidant signalling and dysregulation of iron metabolism are a pathological hallmark of FCD IIb and TSC. Our findings suggest novel therapeutic strategies aimed at controlling the pathological link between both processes.

Keywords

epilepsy; oxidative stress; focal cortical dysplasia; tuberous sclerosis complex; haem oxygenase 1; iron metabolism

Introduction

A hallmark seen in resected brain tissue of patients suffering from acquired forms of epilepsy, such as temporal lobe epilepsy (TLE), is the excessive generation of reactive oxygen species (ROS) that leads to oxidative stress (OS) (1–3). Recently, we showed for the first time strong expression of OS markers, in particular the light chain and catalytic cysteine/glutamate antiporter of the x_c system (SLC7A11 referred to as xCT), in resected brain tissue of patients suffering from epileptogenic developmental malformations, namely focal cortical dysplasia (FCD) type IIb and tuberous sclerosis complex (TSC) (4). Histopathological hallmarks of both pathologies include cortical dyslamination, presence of dysmorphic neurons and large, improperly developed immature cells called balloon cells in FCD IIb or giant cells in TSC (5, 6). Both pathologies represent mTORopathies, characterized by increased cellular mammalian target of rapamycin (mTOR) activation due to mutations in genes in this signalling pathway, which leads to the generation of brain lesions and epileptogenesis (7). Despite advances in understanding the contribution of mTOR hyperactivation to the pathogenesis of TSC and FCD IIb and initial clinical trials of mTOR inhibitors in TSC (8–10), more specific pathogenic alterations that could be targeted by pharmacotherapy remain to be identified. More specifically, only a subset of cells display mTOR hyperactivation making cell specific therapeutics preferable over broad-spectrum mTOR inhibitors, particularly during brain development.

Prior studies demonstrated that overexpression of an essential enzyme in the synthesis of the primary intracellular anti-oxidant glutathione, glutathione-cysteine ligase catalytic subunit (GCLC), is required for redox adaptation and growth advantage of maldeveloped cells in TSC (11). Another study identified increased endoplasmic reticulum stress in TSC and indications for an increase in the activation of OS responsive genes (12). Collectively, these findings suggest that the cellular substrate for mTORopathies display increased OS coupled

with increased OS resistance. Interestingly, expression of components of glutathione synthesis are directly regulated by the nuclear factor erythroid 2 like 2 (NFE2L2 referred to as Nrf-2) transcription factor, a master regulator of the cellular response to OS (13, 14). Upon OS, Nrf-2 activates many genes with cytoprotective roles, i.e. xCT and GCLC. Another important Nrf-2 target is haem oxygenase 1 (HO-1), an enzyme responsive to a variety of pro-inflammatory and pro-oxidant stimuli. It catabolizes potentially pro-oxidant haem into radical scavenging and anti-inflammatory bilirubin making it an important enzyme in first line cellular defence against OS and xenobiotics (15–17).

Since the presence of OS and overexpression of xCT and GCLC are consistent findings in TSC and FCD IIb we were interested if the Nrf-2 pathway is chronically active and if its activation has protective or pathogenic implications. Additionally, we were interested in what disease-relevant mechanisms could lead to sustained activity of this pathway. Here, we were particularly interested in microRNA-155 (miR155) as it is upregulated in TLE and TSC, as well as in different rat models of epileptogenesis, all suggesting an important role for miR155 in epilepsy and epileptogenesis (18–21). Moreover, miR155 was previously shown to be implicated in the regulation of OS in endothelial cells (22, 23).

The aim of this study was to investigate cellular damage due to OS and Nrf-2 activation in TSC and FCD IIb and elucidate the potential contribution of miR155. Moreover, we were interested in changes in iron metabolism due to its potentially pathogenic interaction with ROS and because mTOR is a master regulator of a variety of metabolic processes. To this extent, we used surgically resected brain tissue from patients with drug-resistant epilepsy due to FCD IIb or TSC and a mouse epilepsy model based on conditional *Tsc1* deletion in glial fibrillary acidic protein (GFAP) expressing cells ($Tsc1^{GFAP-/-}$ mice) to investigate these interactions. Finally, we overexpressed miR155 *in vitro* in human foetal astrocytes to investigate the mechanistic link between the factors involved.

Materials & Methods

Subjects

The cases included in this study were obtained from the archives of the departments of Neuropathology of the Amsterdam UMC (Amsterdam, the Netherlands) and the University Medical Center Utrecht (UMCU, Utrecht, the Netherlands). Cortical brain samples were obtained from patients undergoing surgery for drug-resistant epilepsy and diagnosed with FCD IIb (n=8) or TSC (n=14). All cases were reviewed independently by two neuropathologists, and the diagnosis of FCD was confirmed according to the international consensus classification system proposed for grading FCD (5). All patients with cortical tubers fulfilled the diagnostic criteria for TSC (6). None of the FCD patients fulfilled the diagnostic criteria for TSC. Control material was obtained at autopsy from age-matched controls, without a history of seizures or other neurological diseases. All autopsies were performed within 24 h after death. Tissue was obtained and used in accordance with the Declaration of Helsinki and the Amsterdam UMC Research Code provided by the Medical Ethics Committee. Clinical information about the patients can be found in Supp. Tab. 1. Details on immunohistochemistry and molecular analysis are described in the supplementary methods.

Tsc1 $^{GFAP-/-}$ mice

All animal experiments in this study were approved by the Washington University Animal Welfare committee. *Tsc1*$^{flox/flox}$-GFAP-Cre knockout (*Tsc1*$^{GFAP-/-}$) mice with conditional inactivation of the *Tsc1* gene in astrocytes and neurons were generated as described previously (24, 25). *Tsc1*$^{flox/+}$-GFAP-Cre and *Tsc1*$^{flox/flox}$ littermates have previously been found to have no abnormal phenotype and were used as controls in these experiments. Whole cortex and hippocampus were collected from 2-week-old and 2-month-old animals (n=5 animals per group). These time points were chosen on the basis of a previous study in which the course of seizure development in this model was carefully analysed and it was concluded that earliest seizure onset is at 4 weeks of age with a dramatic progressive increase in seizure incidence and frequency at 6 weeks (26). Thus, to investigate the epileptogenic process at time points before and after the development of seizures in this model 2-week-old and 2-month-old *Tsc1*$^{GFAP-/-}$ mice were compared in the present study. For quantitative real-time PCR, tissues were mechanically minced and homogenized in Qiazol Lysis Reagent (Qiagen Benelux, Venlo, the Netherlands). Subsequent RNA isolation was done using the miRNeasy Mini kit (Qiagen Benelux, Venlo, the Netherlands) according to the manufacturer's instructions. For immunohistochemistry, perfusion fixation was performed with 4 % paraformaldehyde, brains were dissected and embedded in paraffin, and processed as described in the supplementary methods.

Transfection and stimulation of cell cultures

Human fetal astrocytes enriched cultures were established as described in the supplementary methods. Maximum tolerable doses of H_2O_2 and glucose oxidase (GO) were determined in fetal astrocyte-enriched cultures with the 3-(4,5-dimethylthiazol-2-yl)-2,5-diphenyl tetrazolium bromide (MTT, Sigma-Aldrich, St Louis, MO, USA) cell viability assay (Supp. Fig. 1). Briefly, cells were treated with different concentrations of H_2O_2 (Sigma-Aldrich, St Louis, MO, USA) or GO from *Aspergillus niger* (type II; Sigma-Aldrich, St Louis, MO, USA) in complete culture medium for 3 h or 72 h, respectively. To ensure maximum activity, stimulation medium containing GO was refreshed every 24 h. Subsequently, 0.5 mg/ml MTT reagent in complete medium was added to each well and cells were incubated for 1 h at 37 °C and 5 % CO_2. Thereafter the reaction mixture was discarded and 100 µl acid isopropanol (4 mM HCl, 0.1 % NP-40 in isopropanol) was added to each well to stop colour development and solubilize cells. Cell density was determined by measuring spectrophotometric absorbance at 570 nm using a microplate reader (BMG Labtech, Ortenberg, Germany).

For transfection, cultures were transfected with either mimic negative control (Suppl. Fig. 1), miR155 mimic (Applied Biosystems, Carlsbad, CA, USA) or antisense miR155 LNA oligonucleotide (miR155 antagomiR, Ribotask ApS, Odense, Denmark) (Supp. Tab 2). Oligonucleotides were delivered to the cells using Lipofectamine® 2000 transfection reagent (Life Technologies, Grand Island, NY, USA) at a final concentration of 50 nM for a total of 24 h and subsequently stimulated with H_2O_2 (3 h) or GO (72 h), respectively. Before harvesting cells for quantitative real-time PCR and Western blot analysis, cells were washed twice with PBS.

Statistical analysis

Statistical analysis of cell culture experiments was performed with GraphPad Prism software version 5.01 (Graphpad software Inc., La Jolla, CA, USA) using the non-parametric Mann-Whitney U test or, for multiple groups, the non-parametric Kruskal-Wallis test with correction for multiple comparisons (Dunn's method). $P<0.05$ was assumed to indicate a significant difference. Data are presented as box plots for human and mouse data and mean ± SEM for cell culture data. For RNA-Seq data (Suppl. methods) a Mann-Whitney U test followed by a Benjamini-Hochberg correction for multiple comparison test was carried out. An adjusted p-value<0.05 was assumed to indicate statistical significance.

Data availability

The data that support the findings of this study are available from the corresponding author, upon reasonable request.

Results

Oxidative stress damage, Nrf-2 activation and miR155 expression in FCD IIb and TSC

To prove the presence of OS damage and activation of Nrf-2 signalling in the epileptogenic pathologies FCD IIb and TSC, we assessed the expression of the OS damage marker 4-hydroxynonenal (4-HNE), the DNA damage marker phosphorylated H2A histone family member X (γH2A.X), as well as the expression of Nrf-2 and HO-1. The immunoreactivity score was increased for all markers in FCD IIb and TSC compared to control (Tab. 1). For the evaluation of immunohistochemical staining in FCD IIb and TSC tissue, cellular morphology was classified as glia (small nucleus and small soma), dysmorphic neurons (big central nucleus with enlarged soma and sometimes non-polarized neurites) and giant/balloon cells (enlarged cells with glassy cytoplasm and laterally displaced nucleus) (see also (5)). Expression of 4-HNE was observed in control brain tissue, mainly in cortical neurons and glia (Fig. 1A). 4-HNE reactivity in FCD IIb and TSC was observed especially in dysmorphic neurons and cells with glial morphology, but also in balloon/giant cells (Fig. 1B, C). Moreover, all cell types showed nuclear γH2A.X reactivity in FCD IIb and TSC tissue as compared to control where it was virtually absent (Fig. 1D–F, Suppl. Fig. 2). Nrf-2 expression was found in cortical neurons and glia in control tissue, while expression in FCD IIb and TSC was located predominantly in the nucleus, but also in the cytoplasm of dysmorphic neurons and balloon/giant cells (Fig. 1G–I). HO-1 expression was detectable in control tissue in neurons and glial cells. In FCD IIb and TSC tissue, HO-1 expression was high in dysmorphic neurons and balloon/giant cells (Fig. 1J–L). In particular, sparsely distributed dysmorphic neurons displayed very strong reactivity (Fig. 1K, L_1). To assess whether HO-1 expression was high in cells with mTOR activation (indicated by pS6 expression) we performed double-labelling with pS6 and HO-1. This revealed HO-1 expression in pS6-positive dysmorphic neurons and balloon/giant cells in FCD IIb and TSC, with strong expression in particular subsets of cells as seen in single labelling (Fig. 1M, N). In addition, HO-1 was also expressed in cells with microglial morphology in 1 case of FCD IIb (Fig. $1M_1$). Perilesional staining displayed similar expression pattern as seen in autoptic control tissue, except for Nrf-2 which was higher (Suppl. Fig. 3).

In previous studies we already found that miR155 expression was higher in TSC tuber tissue as compared to control (19). Here, we wanted to verify this prior finding in an independent TSC cohort and also in a cohort of patients with FCD IIb. *In situ* hybridization revealed mainly neuronal expression of miR155 in the cortex of control tissue with occasional expression in GFAP-positive cells in the WM (Fig. 2A). In FCD IIb and TSC tissue, miR155 expression in dysmorphic neurons was similar to that seen in neurons of control tissue. However, GFAP-positive glial and balloon/giant cells appeared to have stronger miR155 expression as compared to GFAP-positive cells in control tissue (Fig. 2B, C arrowheads). RNA quantification in surgically resected tissue homogenates of TSC patients confirmed stronger expression of miR155 as well as HO-1 as compared to controls (Fig. 2D–F). HO-1 protein was highly expressed in 3 out of 10 patients, while in 7 patients the expression was similar to control (Fig. 2F, representative blot image). In FCD IIb, miR155 was not different to control (Fig. 2G). As in TSC, *HO-1* expression was higher in patients with FCD IIb as compared to controls (Fig. 2H).

Tsc1$^{GFAP-/-}$ mice display high 4-HNE, HO-1 and miR155 expression before the development of spontaneous seizures

To investigate if mTOR hyperactivation *per se* could lead to the expression of 4-HNE, HO-1 and miR155 we analysed expression of these markers in *Tsc1*$^{GFAP-/-}$ mice. Moreover, we compared tissue from mice before and after the onset of seizures to investigate if the expression of these markers preceded seizure development. 4-HNE expression in the hippocampus of control mice was generally low, with slightly higher expression in 2-month-old mice compared to 2-week-old animals (Fig. 3A, C). In contrast, 2-week-old *Tsc1*$^{GFAP-/-}$ mice displayed higher 4-HNE expression in the hippocampus before the development of seizures (Fig. 3B, I, J) which was even stronger in the cortex of 2-month-old *Tsc1*$^{GFAP-/-}$ mice with recurrent seizures (Fig. 3D, I, J). Here, 4-HNE reactivity was predominantly detected in GFAP positive cells and occasionally NeuN positive cells (Fig. 3B_1–B_3, D_1–D_3). HO-1 expression could be detected in all cell types in the hippocampus and cortex of control mice and there was no difference in expression between 2-week-old and 2-month-old control animals (Fig. 3E, G). In contrast, HO-1 expression was very high in a small number of cells with glial morphology before seizure development (Fig. 3F, arrowheads and inserts F_1, H_1). The number of cells displaying very strong HO-1 reactivity was higher after the development of seizures in cortex and hippocampus (Fig. 3F, H, K). Since only cells with glial morphology were strongly HO-1 reactive we wanted to know if these cells were astrocytes (positive for GFAP) or microglia (positive for Iba-1). Double-labelling revealed that cells displaying very strong HO-1 reactivity were GFAP-, but not Iba-1- positive (Fig. 3F_2, F_3, H_2, H_3), however, Iba-1-positive cells were often in close proximity to cells expressing high HO-1. RNA quantification revealed higher expression of miR155 and *HO-1* in the hippocampus and cortex of *Tsc1*$^{GFAP-/-}$ mice compared to wild-type before seizure development, which displayed an even higher fold change compared to control after seizure development (Fig. 3L–O).

In vitro prolonged activation of HO-1 can be induced by miR155 and promotes expression of iron response genes

We detected high HO-1 expression in TSC, FCD IIb and *Tsc1*$^{GFAP-/-}$ mice, thus we were interested whether HO-1 is upregulated in both acute and prolonged OS and if this is accompanied by other pathogenic changes that are seen in TSC. Acute OS in human foetal astrocytes induced upregulation of *HO-1* and *xCT* (Fig. 4A). In contrast, TLR4 signalling components *TLR4* and *TAB-2* were downregulated while *MYD88* did not change. Chronic OS likewise induced *HO-1* and *xCT* expression, however, the relative increase in *HO-1* was less than in acute OS. Moreover, the expression of *TLR4*, *TAB-2* and *MYD88* was higher in response to chronic OS (Fig. 4A). To prove that OS can induce DNA double strand damage as we detected in TSC and FCD IIb we investigated γH2A.X expression in foetal astrocytes and found a marked increase in response to acute OS (Fig. 4B_1–B_3).

Additionally, we were interested if miR155, which we showed previously to be upregulated and to contribute to the inflammatory phenotype in astrocytes, could modulate OS-reactive genes like HO-1. Overexpression of miR155 in astrocytes led to higher expression of *HO-1* and *xCT*, while the expression of BTB domain and CNC homolog 1 (*Bach-1*), a putative miR155 target, was lower. These effects became stronger the longer cells were exposed to miR155 mimic but displayed only minor differences in the presence or absence of OS (Fig. 4C–E). In addition to RNA, the expression of HO-1 protein was higher after miR155 transfection and this could also be replicated in cultured astrocytes derived from surgically resected tissue of TSC patients (Fig. 4H, I). Importantly, the expression was similar to controls when transfection with the miR155 inhibitor was performed. Since we previously found miR155 to exert pro-inflammatory effects, anti-inflammatory HO-1 activity could potentially alleviate these effects. However, HO-1 activity also releases iron, which can potentially exacerbate OS by producing more reactive radicals via the Fenton reaction. Therefore, we analysed iron regulatory genes in response to miR155 dependent chronic HO-1 expression. Chronic, but not acute, exposure of human fetal astrocytes to miR155 induced expression of ferritin heavy chain 1 (*FTH-1*) and *FP-1* (Fig. 4F, G). Additionally, chronic exposure to miR155 made human foetal astrocytes more susceptible to a H_2O_2 challenge with a reduction to 70% viability compared to 90% in control and miR155 inhibitor transfected cells (Fig. 4J). Finally, to investigate if endogenous HO-1 expression in response to OS increases iron levels indicated by the surrogate marker ferritin, independent of miR155, we employed a time-course of H_2O_2 stimulation. Foetal astrocytes exposed to H_2O_2 for different time-points displayed rapid induction of HO-1 protein expression 3 h after stimulation with maximum expression after 6h and a decrease after 24 h. In parallel there was a slightly delayed ferritin induction after 6 h and remained elevated even after 24 h (Fig. 4K).

Increased ferritin expression and altered iron metabolism persists in FCD IIb, TSC and *Tsc1*$^{GFAP-/-}$ mice

Since our *in vitro* data suggested that prolonged activation of anti-oxidant pathways and HO-1 activity induced ferritin, likely due to iron release, we investigated ferritin and other markers of iron metabolism in resected epileptogenic brain tissue of patients with FCD IIb, TSC as well as in *Tsc1*$^{GFAP-/-}$ mice. Ferritin expression in autopsy control brain tissue was

found exclusively in cells with microglial morphology and was very rarely detected in neurons (Fig. 5A). In contrast, dysmorphic neurons and balloon/giant cells in FCD IIb and TSC displayed higher expression (Fig. 5B, C). Importantly, this high expression was found in most but not all cells, some of which were negative for ferritin (Fig. $5B_1$). Total ferritin protein was higher, however, similar to HO-1 only a subset of 4 out of 10 cases had very high expression, whereas the rest showed moderately higher expression compared to control (Fig. 5D). Double-labelling with pS6 showed consistent co-localization with ferritin in most cells, however, pS6-positive ferritin-negative cells were also present in FCD IIb and TSC (Fig. 5E, F, E_1, F_1 red cells). RNA expression revealed higher expression of ferritin light chain (*FTL*) and *CP* in TSC and *TF* and *CP* in FCD IIb (Fig. 5G, H). *FP-1* protein expression was not changed in TSC (Fig. 5I). RNA expression in *Tsc1*$^{GFAP-/-}$ mice displayed higher expression of *FTH-1* and *FP-1* before typical seizure onset and higher *CP* expression after seizure onset in the cortex. In the hippocampus, *FTH-1*, *TF*, *CP* and *FP-1* expression was higher only after seizure onset (Fig. 5J–M).

High 4-HNE, HO-1 and ferritin appear during TSC brain development and become cell-specific in adolescent patients.

We were interested if 4-HNE, HO-1 and ferritin expression precede seizure development not only in *Tsc1*$^{GFAP-/-}$ mice, but also affect cells during brain development in TSC. Moreover, we wanted to know how the expression pattern changes over time, thus we compared fetal TSC brain tissue to resected brain tissue from adolescent TSC patients. TSC tissue from fetal TSC brain (f, 27 gestational weeks (GW), TSC2 and f, 32 GW, TSC2) displayed 4-HNE reactivity predominantly in fetal giant cells (Fig. 6A). In comparison, tubers of adolescent TSC patients (13 and 24 years old) displayed 4-HNE reactivity in giant cells and cells with glial morphology, but only in a few dysmorphic neurons (Fig. 6B). Expression of HO-1 was very high in giant cells in fetal TSC tissue displaying highly reactive intracellular inclusions (Fig. 6C, arrowheads). Lesions from adolescent TSC patients revealed the same HO-1 expression pattern as seen in Fig. 1 with high expression in dysmorphic neurons and giant cells (Fig. 6D). Ferritin expression in fetal TSC brain tissue was found in most neural precursor cells (Fig. 6E) with some displaying weak expression (Fig. $6E_1$). In resected brain tissue from adolescent TSC patients, ferritin expression was found in dysmorphic neurons, giant cells and cells with glial morphology (Fig. 6F, F_1). Overall, expression of all three markers was already high in neural precursor cells during cell migration and proliferation (Fig. 6C, E). In the adolescent TSC brain, the expression remained high, but the number of positive cells was lower and became more cell type specific with increasing cellular differentiation (Fig. 6F). To generalize the dysregulation of antioxidant genes and genes in iron metabolism in TSC we re-analysed RNA sequencing data from an independent TSC cohort from a previous report (27). We found similar expression patterns for both pathways indicating a general upregulation of anti-oxidant and iron regulatory genes (Fig. 6G). Interestingly, autoptic tissue from the only two old control subjects (39 y and 44 y; Fig. 6G, arrows) displayed activation of both pathways similar to TSC tissue, indicating an age dependent increase in healthy individuals.

Discussion

We report evidence that TSC and FCD IIb are characterized by OS, chronic Nrf-2 activation and provide indications that redox state and iron metabolism are altered in both these developmental malformations related to mTOR dysregulation. Moreover, our results suggest that these processes are present prior to seizure development and could contribute to epileptogenesis. Finally, our results imply that miR155 may contribute to Nrf-2 activation and HO-1 expression.

We previously identified that markers of OS are increased in TLE (3) as well as in malformations of cortical development (4). However, we did not investigate directly if malformations of cortical development also harbour cellular damage, which we prove here by showing higher lipid peroxidation and DNA double strand damage in TSC and FCD IIb brain tissue. Consistent with this, we see γH2A.X reactivity in acute OS *in vitro*. Interestingly, HO-1 and 4-HNE expression were highest in dysmorphic neurons and giant/balloon cells in TSC, FCD IIb and in astrocytes of $Tsc1^{GFAP-/-}$ mice. Since mTOR activation persists in the brain of patients with TSC and FCD IIb and in astrocytes in $Tsc1^{GFAP-/-}$ mice it is interesting that only a subset of cells with mTOR activation display strong HO-1 expression. This suggests secondary mechanisms, other than only mTOR hyperactivity are necessary to induce sustained HO-1 expression. One possible secondary mechanism could be the presence of positive modulators such as miR155. Since miR155 expression can be induced by inflammation and immune responses its expression might also be driven by the same processes in TSC and FCD IIb (28). Importantly, we confirmed upregulation of miR155 in TSC tubers from a previous cohort (19) and show here for the first time higher miR155 expression prior to seizure development in $Tsc1^{GFAP-/-}$ mice. We could not detect higher expression in FCD IIb tissue, which might be due to cell type specific regulation or a lower fraction of cells with mTOR activation in FCD IIb lesions compared to TSC that cannot be detected on bulk tissue analysis. Mechanistically, *in vitro* human fetal astrocytes and TSC-derived astrocytes transfected with miR155 show high expression of Nrf-2 targets HO-1 and xCT likely by miR155 dependent inhibition of the Nrf-2-competitive transcription factor Bach-1 (29, 30). While miR155 can clearly modulate Nrf-2 activity *in vitro*, we also believe that other factors in TSC and FCD IIb contribute to the expression of HO-1, since it is an acute phase protein. This is also reflected by the discrepancy between HO-1 RNA and protein expression on Western blot indicating post-transcriptional regulatory processes as shown previously (31). One example of post-transcriptional control is miR155, which could have important implications in modulating sustained HO-1 expression.

Nrf-2 signalling and HO-1 expression upon OS might help to defend the brain, resolving OS and inflammation. On the other hand, prolonged activity due to OS might be detrimental or contribute to pathogenesis in TSC and FCD IIb. To investigate the difference between acute and chronic Nrf-2 activation we stimulated foetal astrocytes with H_2O_2 for 3 h or GO for 72 h *in vitro*. We observed HO-1 upregulation upon OS in both conditions. However, while we measured a reduction in several genes of the pro-inflammatory NF-κB signalling pathway upon acute OS, likely via HO-1 anti-inflammatory action (32, 33), chronic OS led to higher expression of the very same genes. These results suggest a transient anti-inflammatory effect

of HO-1 in response to pro-oxidant stimuli that is replaced by secondary, pro-inflammatory signalling cascades when chronically active (34). Therefore, we hypothesize that prolonged, excessive HO-1 expression does not directly serve the anti-inflammatory and anti-oxidant purpose it does acutely. The potentially detrimental role of HO-1 is supported by the increase in ferritin expression, a surrogate marker for intracellular iron concentrations, in fetal astrocytes chronically transfected with miR155. This effect likely results from haem-derived free iron deposition via HO-1. While we observed that HO-1 expression is always accompanied by ferritin expression, likely to buffer released iron that otherwise participates in the Fenton reaction with H_2O_2 to produce even more reactive radicals, HO-1 is rapidly suppressed again. However, cells with sustained miR155 dependent HO-1 expression are more susceptible to OS due to excess iron, leading to cell death. These observations are in agreement with studies showing that sustained HO-1 activation can participate in oxidative modification of macromolecules via pro-oxidant, labile iron (35–38).

In addition to HO-1, the Nrf-2 target xCT was shown to be upregulated in glia, dysmorphic neurons and giant/balloon cells in TSC and FCD IIb (4). In the present study we could show *in vitro* that miR155 dependent Nrf-2 stimulation also increases the expression of xCT. In the context of epilepsy and neuronal discharges increased extracellular glutamate provides an important determinant of xCT activity, which transports cysteine, the limiting amino acid in glutathione synthesis, in exchange for glutamate across membranes. In turn, high extracellular glutamate shifts the concentration gradient necessitating increased xCT expression for glutathione synthesis. Hence, cells expressing more xCT might be resistant to glutamate-dependent excitotoxic OS. Intriguingly we see xCT overexpression in dysmorphic cells in TSC and FCD IIb, as well as in TLE (3) and these result synergize with previous reports showing that GCLC, another component of glutathione metabolism, is necessary for redox adaptation and aberrant cell growth in TSC2 mutant cells (11). Besides ferritin, we also detected specific RNA induction of the iron exporter *FP-1* in foetal astrocytes chronically transfected with miR155, however, only in OS conditions. This suggests an increased necessity to secrete excess iron produced by HO-1, specifically in pro-oxidant conditions. In human TSC and FCD IIb brain tissue we detected higher RNA expression of ferritin, *TF* and *CP*, while FP-1 protein expression was not changed. Although ferritin can sequester labile free iron, it was also shown that iron can be released again from ferritin in OS conditions (39, 40). The net effect of these changes suggests increased iron availability to cells, potentially further increasing the intracellular labile iron pool in addition to haem-derived iron due to HO-1 activity. Besides human tissue we also detected higher *FTH-1*, *TF*, *CP* and *FP-1* RNA in *Tsc1*$^{GFAP-/-}$ mice indicating changes in iron metabolism. Importantly, higher *FTH-1* and *FP-1* expression together with OS and HO-1 expression precedes seizure development in the cortex of these mice. This is also seen in foetal TSC brain, in which neural precursor cells display dysregulated HO-1 and ferritin expression together with 4-HNE reactivity before birth and the formation of tubers. Importantly, we analysed an independent TSC cohort which supported upregulation of anti-oxidant and iron regulatory genes, suggesting that this effect is a common phenomenon in TSC. All of these findings indicate a complex interconnection of mTOR, anti-oxidant genes and iron regulatory genes, summarized in Fig. 6h.

Considering high iron concentrations in the majority of dysmorphic cells in FCD IIb and TSC lesions, targeting these subsets of cells with ferroptotic agents might represent a promising novel treatment option. Ferroptosis is a regulated form of cell death due to iron dependent excessive lipid peroxidation (41). Here, HO-1 was shown to be an essential component, with prolonged, excessive activation promoting cell death (42–45). Ferroptosis-mediated cell death ensues only when the intracellular defence mechanisms against lipid peroxidation and iron overload are overwhelmed. Key components in resistance to ferroptosis represent iron sequestering proteins like ferritin and proteins in thiol metabolism that provide the basis for anti-oxidant glutathione synthesis, in particular xCT and glutathione peroxidase 4 (GPx4) which is important in detoxification of lipid peroxides and essential for neuronal survival (46–48). Since prior studies verified increased expression of xCT and GCLC in TSC (4, 11), dysmorphic cells in TSC and FCD IIb likely increase Nrf-2 activity to adapt to increased intracellular iron caused by mTOR activity, while paradoxically producing even more labile iron via HO-1. While it was shown that increase mTOR activity makes cells more susceptible to apoptotic cell death (49, 50), ferroptosis might be another important contributor to cell loss during brain development in TSC patients. Indeed, we find evidence for prominent cell loss in postnatal tissue from FCD IIb and TSC subjects (51, 52). This suggests possible ongoing ferroptotic cell loss and redox adaptation, even after birth, further exacerbated by seizure activity. In essence, these processes could create a strong positive selection pressure for cells with resistance to OS and excess iron and indicate that pharmacotherapy targeting iron homeostasis or redox adaptation could be exploited to specifically target dysmorphic cells. Finally, it is generally believed that aberrant network formation in FCD IIb and TSC not only gives rise to epilepsy but also the frequently observed cognitive impairments (53–55). Interestingly, evidence from other pathologies like Alzheimer's disease suggests that iron accumulation might act as driver of cognitive deterioration by ferroptosis, OS or related inflammatory responses (56). Thus, disturbed iron homeostasis and iron overload could represent a common neuropathological mechanism underlying both, epilepsy and cognitive comorbidities in FCD IIb and TSC. We propose that therapeutics inhibiting redox or iron adaptation, such as Nrf-2 inhibitors or ferroptotic agents, might have therapeutic value to specifically target a subset of pathogenic cells in TSC and FCD IIb. Additionally, this approach could circumvent side effects of current mTOR inhibitors. Moreover, these findings may have important implications in other selected sub-types of epilepsy with dysregulation of anti-oxidant signalling and iron metabolism (such as TLE and other acquired focal epilepsies) and may yield new therapeutic strategies aimed at controlling the pathological link between oxidative stress, inflammation and the dysregulated iron metabolism, common neurobiological mechanisms underlying epilepsy and cognitive and behavioural comorbidities.

Supplementary Material

Refer to Web version on PubMed Central for supplementary material.

Acknowledgments

TSZ, GC, AA, AK and JDM performed the experiments, data collection and analysis. WvH, WGS, PCvR, JCB, SI and EA helped with the selection and collection of human brain tissues and clinical data. NRR and MW collected *Tsc1*GFAP$^{-/-}$ mouse tissue. EA, EAvV and JDM conceived the study and participated in its design and

coordination. TSZ, JDM, EAvV and EA drafted and prepared the manuscript. All authors read, revised, and approved the final manuscript. The research leading to these results has received funding from the European Union's Seventh Framework Programme (FP7/2007–2013) under grant agreement no. 602391 (EPISTOP; EA, FJ) and no. 602102 (EPITARGET; EAvV, EA), the Dutch Epilepsy Foundation, project number 16–05 (EAvV), the European Union's Horizon 2020 Research and Innovation Programme under the Marie Sklodowska-Curie grant agreement no. 642881 (ECMED; AK, EA) and no. 722053 (EU-GliaPhD; TS, EA), and the United States National Institutes of Health NS056872 (MW).

Abbreviations

4-HNE	4-hydroxynonenal
γH2A.X	phosphorylated H2A histone family member X
Bach-1	BTB domain and CNC homolog 1
CAT	catalase
CP	ceruloplasmin
FCD IIb	focal cortical dysplasia type IIb
FPKM	fragments per kilobase million
FTH1	ferritin heavy chain 1
FTL	ferritin light chain
GCLC	glutathione-cysteine ligase catalytic subunit
GCLM	glutamate-cysteine ligase modifier subunit
GFAP	glial fibrillary acidic protein
GO	glucose oxidase
GPX4	glutathione peroxidase 4
HO-1	haem oxygenase 1
LTF	lactotransferrin
miR155	microRNA-155
mTOR	mammalian target of rapamycin
MTT	3-(4,5-dimethylthiazol-2-yl)-2,5-diphenyl tetrazolium bromide
Nrf-2	nuclear factor erythroid 2 like 2
OS	oxidative stress
PBS	Phosphate Buffered Saline
RNA-Seq	RNA-Sequencing
ROS	reactive oxygen species

SOD	superoxide dismutase
TSC	tuberous sclerosis complex
TF	transferrin
TLE	temporal lobe epilepsy
xCT	catalytic cysteine/glutamate antiporter of the x_c system; (*SLC7A11*)

References

1. Martinc B, Grabnar I, Vovk T. The role of reactive species in epileptogenesis and influence of antiepileptic drug therapy on oxidative stress. Curr Neuropharmacol. 2012;10(4):328–43. [PubMed: 23730257]
2. Shin EJ, Jeong JH, Chung YH, Kim WK, Ko KH, Bach JH, et al. Role of oxidative stress in epileptic seizures. Neurochem Int. 2011;59(2):122–37. [PubMed: 21672578]
3. Pauletti A, Terrone G, Shekh-Ahmad T, Salamone A, Ravizza T, Rizzi M, et al. Targeting oxidative stress improves disease outcomes in a rat model of acquired epilepsy. Brain. 2019.
4. Arena A, Zimmer TS, van Scheppingen J, Korotkov A, Anink JJ, Muhlebner A, et al. Oxidative stress and inflammation in a spectrum of epileptogenic cortical malformations: molecular insights into their interdependence. Brain Pathol. 2018.
5. Blumcke I, Thom M, Aronica E, Armstrong DD, Vinters HV, Palmini A, et al. The clinicopathologic spectrum of focal cortical dysplasias: a consensus classification proposed by an ad hoc Task Force of the ILAE Diagnostic Methods Commission. Epilepsia. 2011;52(1):158–74. [PubMed: 21219302]
6. Samueli S, Abraham K, Dressler A, Groeppel G, Jonak C, Muehlebner A, et al. Tuberous Sclerosis Complex: new criteria for diagnostic work-up and management. Wien Klin Wochenschr. 2015;127(15–16):619–30. [PubMed: 25860851]
7. Crino PB. mTOR signaling in epilepsy: insights from malformations of cortical development. Cold Spring Harb Perspect Med. 2015;5(4).
8. Krueger DA, Care MM, Holland K, Agricola K, Tudor C, Mangeshkar P, et al. Everolimus for subependymal giant-cell astrocytomas in tuberous sclerosis. N Engl J Med. 2010;363(19):1801–11. [PubMed: 21047224]
9. Overwater IE, Rietman AB, Bindels-de Heus K, Looman CW, Rizopoulos D, Sibindi TM, et al. Sirolimus for epilepsy in children with tuberous sclerosis complex: A randomized controlled trial. Neurology. 2016;87(10):1011–8. [PubMed: 27511181]
10. French JA, Lawson JA, Yapici Z, Ikeda H, Polster T, Nabbout R, et al. Adjunctive everolimus therapy for treatment-resistant focal-onset seizures associated with tuberous sclerosis (EXIST-3): a phase 3, randomised, double-blind, placebo-controlled study. Lancet. 2016;388(10056):2153–63. [PubMed: 27613521]
11. Malik AR, Liszewska E, Skalecka A, Urbanska M, Iyer AM, Swiech LJ, et al. Tuberous sclerosis complex neuropathology requires glutamate-cysteine ligase. Acta Neuropathol Commun. 2015;3:48. [PubMed: 26220190]
12. Di Nardo A, Kramvis I, Cho N, Sadowski A, Meikle L, Kwiatkowski DJ, et al. Tuberous sclerosis complex activity is required to control neuronal stress responses in an mTOR-dependent manner. J Neurosci. 2009;29(18):5926–37. [PubMed: 19420259]
13. Habib E, Linher-Melville K, Lin HX, Singh G. Expression of xCT and activity of system xc(−) are regulated by NRF2 in human breast cancer cells in response to oxidative stress. Redox Biol. 2015;5:33–42. [PubMed: 25827424]
14. Dickinson DA, Levonen AL, Moellering DR, Arnold EK, Zhang H, Darley-Usmar VM, et al. Human glutamate cysteine ligase gene regulation through the electrophile response element. Free Radic Biol Med. 2004;37(8):1152–9. [PubMed: 15451055]

15. Dore S, Takahashi M, Ferris CD, Zakhary R, Hester LD, Guastella D, et al. Bilirubin, formed by activation of heme oxygenase-2, protects neurons against oxidative stress injury. Proc Natl Acad Sci U S A. 1999;96(5):2445–50. [PubMed: 10051662]
16. Llesuy SF, Tomaro ML. Heme oxygenase and oxidative stress. Evidence of involvement of bilirubin as physiological protector against oxidative damage. Biochim Biophys Acta. 1994;1223(1):9–14. [PubMed: 8061058]
17. Nakagami T, Toyomura K, Kinoshita T, Morisawa S. A beneficial role of bile pigments as an endogenous tissue protector: anti-complement effects of biliverdin and conjugated bilirubin. Biochim Biophys Acta. 1993;1158(2):189–93. [PubMed: 8399320]
18. Ashhab MU, Omran A, Kong H, Gan N, He F, Peng J, et al. Expressions of tumor necrosis factor alpha and microRNA-155 in immature rat model of status epilepticus and children with mesial temporal lobe epilepsy. J Mol Neurosci. 2013;51(3):950–8. [PubMed: 23636891]
19. van Scheppingen J, Iyer AM, Prabowo AS, Muhlebner A, Anink JJ, Scholl T, et al. Expression of microRNAs miR21, miR146a, and miR155 in tuberous sclerosis complex cortical tubers and their regulation in human astrocytes and SEGA-derived cell cultures. Glia. 2016;64(6):1066–82. [PubMed: 27014996]
20. Gorter JA, Iyer A, White I, Colzi A, van Vliet EA, Sisodiya S, et al. Hippocampal subregion-specific microRNA expression during epileptogenesis in experimental temporal lobe epilepsy. Neurobiol Dis. 2014;62:508–20. [PubMed: 24184920]
21. Korotkov A, Broekaart DWM, van Scheppingen J, Anink JJ, Baayen JC, Idema S, et al. Increased expression of matrix metalloproteinase 3 can be attenuated by inhibition of microRNA-155 in cultured human astrocytes. J Neuroinflammation. 2018;15(1):211. [PubMed: 30031401]
22. Chen H, Liu Gao MY, Zhang L, He FL, Shi YK, Pan XH, et al. MicroRNA-155 affects oxidative damage through regulating autophagy in endothelial cells. Oncol Lett. 2019;17(2):2237–43. [PubMed: 30675289]
23. Pulkkinen KH, Yla-Herttuala S, Levonen AL. Heme oxygenase 1 is induced by miR-155 via reduced BACH1 translation in endothelial cells. Free Radic Biol Med. 2011;51(11):2124–31. [PubMed: 21982894]
24. Uhlmann EJ, Wong M, Baldwin RL, Bajenaru ML, Onda H, Kwiatkowski DJ, et al. Astrocyte-specific TSC1 conditional knockout mice exhibit abnormal neuronal organization and seizures. Ann Neurol. 2002;52(3):285–96. [PubMed: 12205640]
25. Zou J, Zhang B, Gutmann DH, Wong M. Postnatal reduction of tuberous sclerosis complex 1 expression in astrocytes and neurons causes seizures in an age-dependent manner. Epilepsia. 2017;58(12):2053–63. [PubMed: 29023667]
26. Erbayat-Altay E, Zeng LH, Xu L, Gutmann DH, Wong M. The natural history and treatment of epilepsy in a murine model of tuberous sclerosis. Epilepsia. 2007;48(8):1470–6. [PubMed: 17484760]
27. Mills JD, Iyer AM, van Scheppingen J, Bongaarts A, Anink JJ, Janssen B, et al. Coding and small non-coding transcriptional landscape of tuberous sclerosis complex cortical tubers: implications for pathophysiology and treatment. Sci Rep. 2017;7(1):8089. [PubMed: 28808237]
28. Elton TS, Selemon H, Elton SM, Parinandi NL. Regulation of the MIR155 host gene in physiological and pathological processes. Gene. 2013;532(1):1–12. [PubMed: 23246696]
29. O'Connell RM, Rao DS, Chaudhuri AA, Boldin MP, Taganov KD, Nicoll J, et al. Sustained expression of microRNA-155 in hematopoietic stem cells causes a myeloproliferative disorder. J Exp Med. 2008;205(3):585–94. [PubMed: 18299402]
30. Yin Q, McBride J, Fewell C, Lacey M, Wang X, Lin Z, et al. MicroRNA-155 is an Epstein-Barr virus-induced gene that modulates Epstein-Barr virus-regulated gene expression pathways. J Virol. 2008;82(11):5295–306. [PubMed: 18367535]
31. Amadio M, Scapagnini G, Davinelli S, Calabrese V, Govoni S, Pascale A. Involvement of ELAV RNA-binding proteins in the post-transcriptional regulation of HO-1. Front Cell Neurosci. 2014;8:459. [PubMed: 25642166]
32. Chhikara M, Wang S, Kern SJ, Ferreyra GA, Barb JJ, Munson PJ, et al. Carbon monoxide blocks lipopolysaccharide-induced gene expression by interfering with proximal TLR4 to NF-kappaB signal transduction in human monocytes. PLoS One. 2009;4(12):e8139. [PubMed: 19956541]

33. Wegiel B, Gallo D, Csizmadia E, Roger T, Kaczmarek E, Harris C, et al. Biliverdin inhibits Toll-like receptor-4 (TLR4) expression through nitric oxide-dependent nuclear translocation of biliverdin reductase. Proc Natl Acad Sci U S A. 2011;108(46):18849–54. [PubMed: 22042868]
34. Suttner DM, Dennery PA. Reversal of HO-1 related cytoprotection with increased expression is due to reactive iron. FASEB J. 1999;13(13):1800–9. [PubMed: 10506583]
35. Song W, Su H, Song S, Paudel HK, Schipper HM. Over-expression of heme oxygenase-1 promotes oxidative mitochondrial damage in rat astroglia. J Cell Physiol. 2006;206(3):655–63. [PubMed: 16222706]
36. Song W, Zukor H, Lin SH, Liberman A, Tavitian A, Mui J, et al. Unregulated brain iron deposition in transgenic mice over-expressing HMOX1 in the astrocytic compartment. J Neurochem. 2012;123(2):325–36. [PubMed: 22881289]
37. Gorter JA, Mesquita AR, van Vliet EA, da Silva FH, Aronica E. Increased expression of ferritin, an iron-storage protein, in specific regions of the parahippocampal cortex of epileptic rats. Epilepsia. 2005;46(9):1371–9. [PubMed: 16146431]
38. Gorter JA, van Vliet EA, Aronica E, Breit T, Rauwerda H, Lopes da Silva FH, et al. Potential new antiepileptogenic targets indicated by microarray analysis in a rat model for temporal lobe epilepsy. J Neurosci. 2006;26(43):11083–110. [PubMed: 17065450]
39. Kaur D, Rajagopalan S, Andersen JK. Chronic expression of H-ferritin in dopaminergic midbrain neurons results in an age-related expansion of the labile iron pool and subsequent neurodegeneration: implications for Parkinson's disease. Brain Res. 2009;1297:17–22. [PubMed: 19699718]
40. Wesselius LJ, Nelson ME, Skikne BS. Increased release of ferritin and iron by iron-loaded alveolar macrophages in cigarette smokers. Am J Respir Crit Care Med. 1994;150(3):690–5. [PubMed: 8087339]
41. Stockwell BR, Friedmann Angeli JP, Bayir H, Bush AI, Conrad M, Dixon SJ, et al. Ferroptosis: A Regulated Cell Death Nexus Linking Metabolism, Redox Biology, and Disease. Cell. 2017;171(2):273–85. [PubMed: 28985560]
42. Adedoyin O, Boddu R, Traylor A, Lever JM, Bolisetty S, George JF, et al. Heme oxygenase-1 mitigates ferroptosis in renal proximal tubule cells. Am J Physiol Renal Physiol. 2018;314(5):F702–F14. [PubMed: 28515173]
43. Hassannia B, Wiernicki B, Ingold I, Qu F, Van Herck S, Tyurina YY, et al. Nano-targeted induction of dual ferroptotic mechanisms eradicates high-risk neuroblastoma. J Clin Invest. 2018;128(8):3341–55. [PubMed: 29939160]
44. Chang LC, Chiang SK, Chen SE, Yu YL, Chou RH, Chang WC. Heme oxygenase-1 mediates BAY 11–7085 induced ferroptosis. Cancer Lett. 2018;416:124–37. [PubMed: 29274359]
45. Kwon MY, Park E, Lee SJ, Chung SW. Heme oxygenase-1 accelerates erastin-induced ferroptotic cell death. Oncotarget. 2015;6(27):24393–403. [PubMed: 26405158]
46. Dixon SJ, Lemberg KM, Lamprecht MR, Skouta R, Zaitsev EM, Gleason CE, et al. Ferroptosis: an iron-dependent form of nonapoptotic cell death. Cell. 2012;149(5):1060–72. [PubMed: 22632970]
47. Yang WS, SriRamaratnam R, Welsch ME, Shimada K, Skouta R, Viswanathan VS, et al. Regulation of ferroptotic cancer cell death by GPX4. Cell. 2014;156(1–2):317–31. [PubMed: 24439385]
48. Yoo SE, Chen L, Na R, Liu Y, Rios C, Van Remmen H, et al. Gpx4 ablation in adult mice results in a lethal phenotype accompanied by neuronal loss in brain. Free Radic Biol Med. 2012;52(9):1820–7. [PubMed: 22401858]
49. Ozcan U, Ozcan L, Yilmaz E, Duvel K, Sahin M, Manning BD, et al. Loss of the tuberous sclerosis complex tumor suppressors triggers the unfolded protein response to regulate insulin signaling and apoptosis. Mol Cell. 2008;29(5):541–51. [PubMed: 18342602]
50. Reith RM, Way S, McKenna J 3rd, Haines K, Gambello MJ. Loss of the tuberous sclerosis complex protein tuberin causes Purkinje cell degeneration. Neurobiol Dis. 2011;43(1):113–22. [PubMed: 21419848]
51. Muhlebner A, Iyer AM, van Scheppingen J, Anink JJ, Jansen FE, Veersema TJ, et al. Specific pattern of maturation and differentiation in the formation of cortical tubers in tuberous sclerosis

omplex (TSC): evidence from layer-specific marker expression. J Neurodev Disord. 2016;8:9. [PubMed: 27042238]

52. Scholl T, Muhlebner A, Ricken G, Gruber V, Fabing A, Samueli S, et al. Impaired oligodendroglial turnover is associated with myelin pathology in focal cortical dysplasia and tuberous sclerosis complex. Brain Pathol. 2017;27(6):770–80. [PubMed: 27750396]
53. Curatolo P, Napolioni V, Moavero R. Autism spectrum disorders in tuberous sclerosis: pathogenetic pathways and implications for treatment. J Child Neurol. 2010;25(7):873–80. [PubMed: 20207609]
54. Curatolo P, Moavero R, de Vries PJ. Neurological and neuropsychiatric aspects of tuberous sclerosis complex. Lancet Neurol. 2015;14(7):733–45. [PubMed: 26067126]
55. Chipaux M, Szurhaj W, Vercueil L, Milh M, Villeneuve N, Cances C, et al. Epilepsy diagnostic and treatment needs identified with a collaborative database involving tertiary centers in France. Epilepsia. 2016;57(5):757–69. [PubMed: 27037674]
56. Ayton S, Wang Y, Diouf I, Schneider JA, Brockman J, Morris MC, et al. Brain iron is associated with accelerated cognitive decline in people with Alzheimer pathology. Mol Psychiatry. 2019.

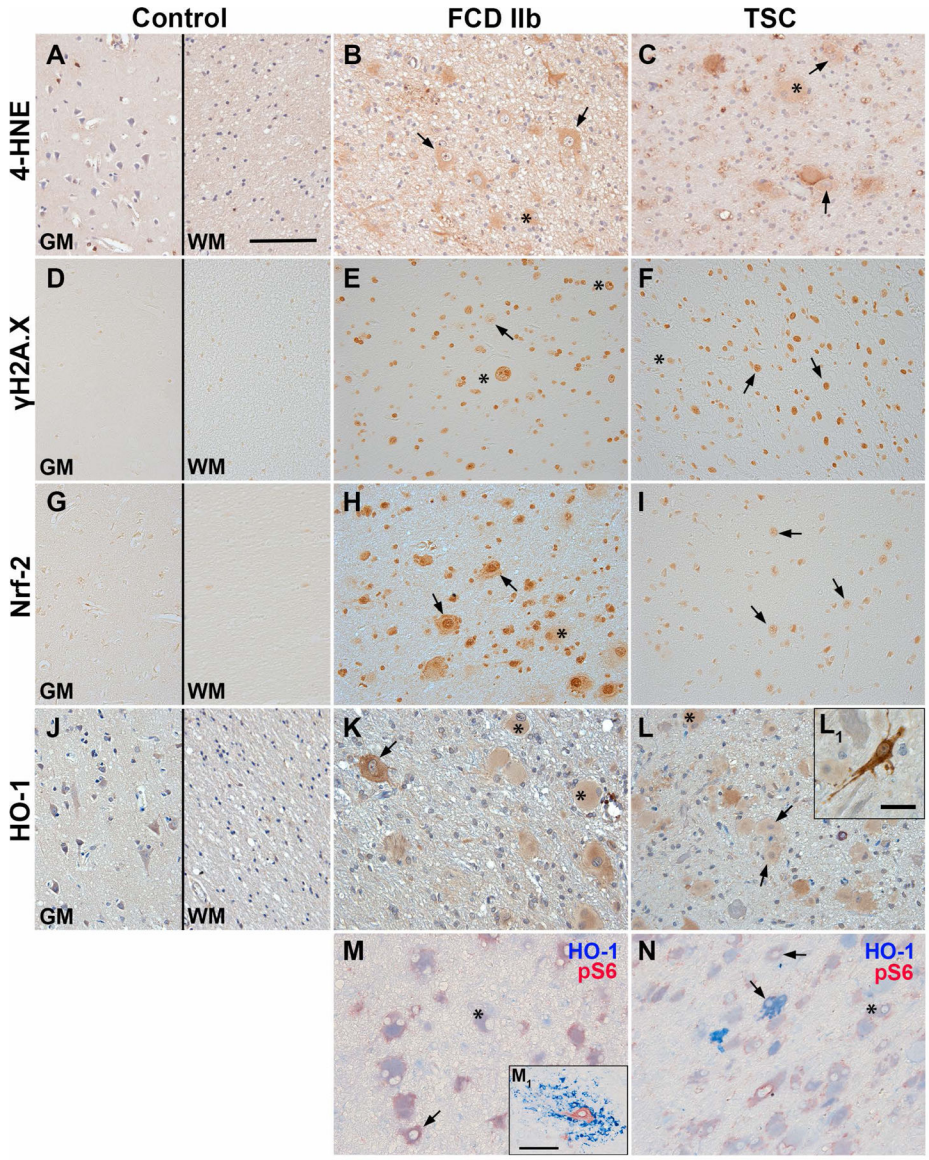

Fig. 1. Higher expression of 4-HNE, γH2A.X, Nrf-2 and HO-1 in TSC and FCD brain specimens.

(**A, D, G, J)** Expression of OS markers in grey (GM) and white matter (WM) of autopsy control tissue. Low 4-HNE and Nrf-2 expression was observed in cells with neuronal and glial morphology in GM of control tissue, whereas γH2A.X was virtually absent in control tissue. HO-1 was moderately expressed primarily in neurons in control GM and WM. (**B, C)** In FCD IIb and TSC 4-HNE immunoreactivity was high in particular in dysmorphic neurons and balloon/giant cells, with higher reactivity in cellular processes surrounding dysmorphic neurons in TSC. **(E, F)** Expression of γH2A.X was much higher in all cell types in FCD IIb and TSC. **(H, I)** Nrf-2 expression was higher in astrocytes and neurons in FCD IIb and TSC as compared to control, particularly in the nucleus. **(K, L)** HO-1 reactivity was high in balloon/giant cells in FCD IIb and TSC tissue, with very high expression in dysmorphic neurons. **(M, N)** Double-labelling with HO-1 revealed consistent co-localization with pS6 in FCD IIb and TSC, while some pS6 positive dysmorphic neurons lacked HO-1 expression

(M_1). High HO-1 expression was predominately found in dysmorphic cells **(L_1)**. One FCD IIb case displayed cells with microglial morphology with very high HO-1 reactivity surrounding dysmorphic neurons **(M_1)**. Sections A–C and J–L were counterstained with haematoxylin, Scale bars: 100 μm in A (representative for A–N), 20 μm in L_1 and 100 μm in M_1; arrows = dysmorphic neurons, asterisk = balloon/giant cells

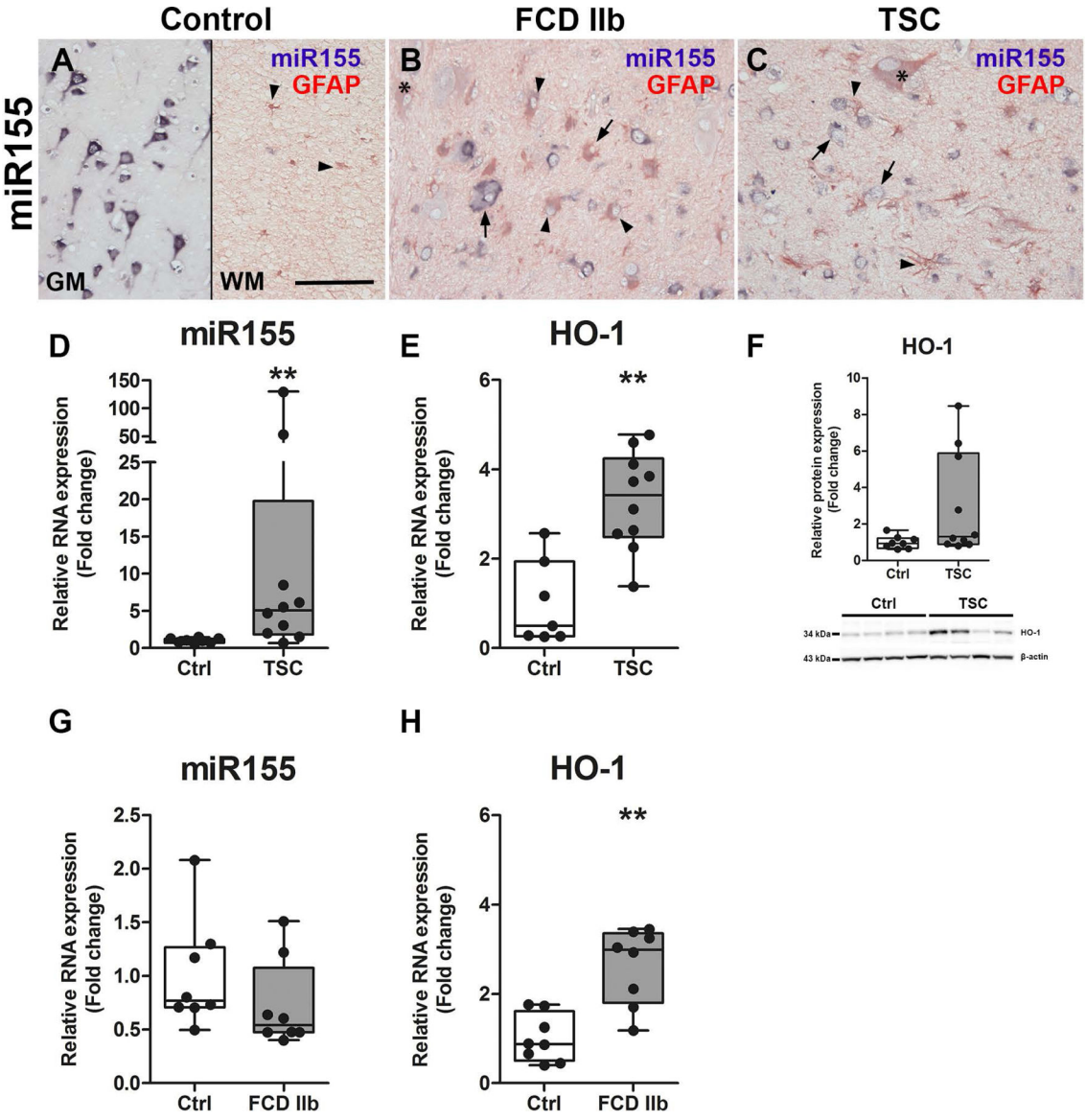

Fig. 2. Higher expression of miR155 and HO-1 in TSC and FCD IIb.

(A) Expression of miR155 was predominately found in neurons of the grey matter (GM) with low expression in glia of the white matter (WM) (arrowheads). **(B, C)** In contrast, miR155 expression was predominantly found in GFAP-positive cells with glial morphology and giant/balloon cells in FCD IIb and TSC as compared to control, whereas expression in dysmorphic neurons did not differ from control. (**D)** Expression of total miR155 in TSC tissue was higher than in control. **(E, F)** Moreover, HO-1 RNA expression was higher in surgically resected tuber tissue from TSC patients compared to autoptic control, while HO-1 protein expression was high only in a subset of patients. **(G, H)** miR155 expression was not different between autopsy control tissue and FCD IIb, while HO-1 RNA was higher. Mann-Whitney U-test. Data are expressed relative to expression observed in controls. Error bars represent range; ** $p<0.01$. n = 8 (Autopsy control, FCD IIb), n = 10 (TSC). Scale bar 100

μm in A (representative for A–C), arrows = dysmorphic neurons, arrowheads = glia, asterisk = balloon/giant cells

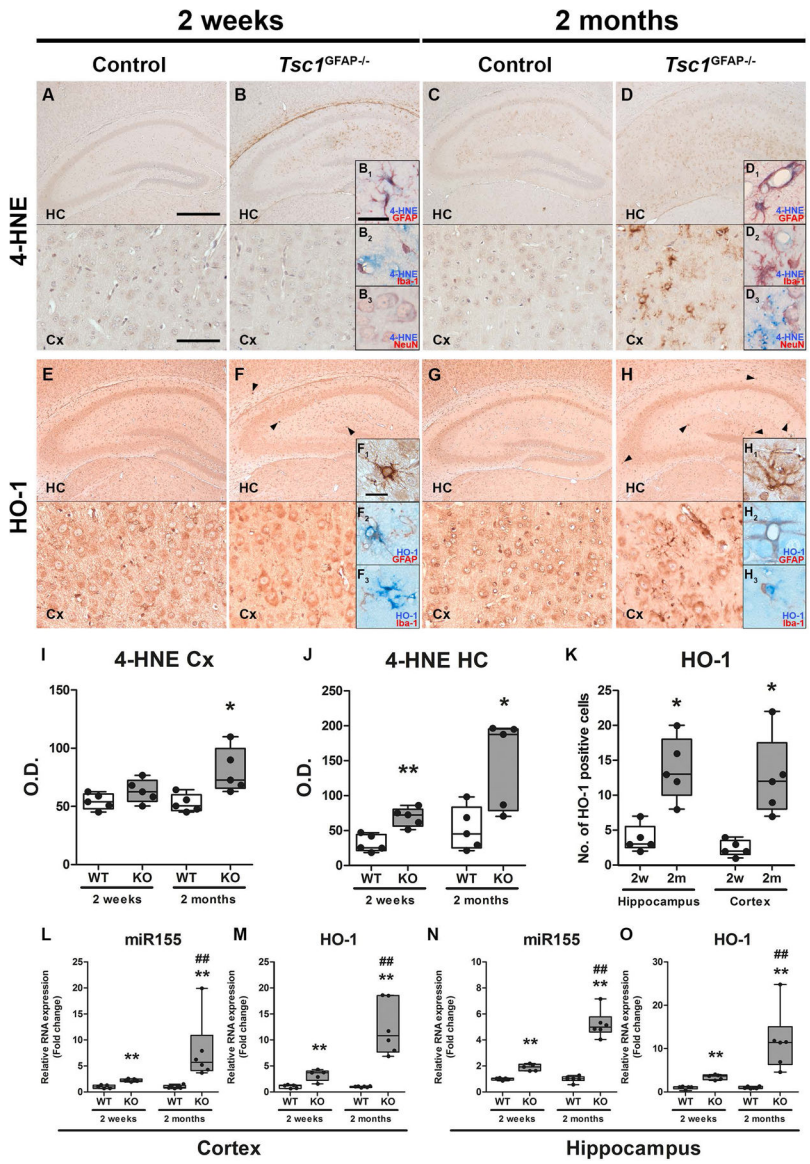

Fig. 3. Higher expression of 4-HNE, HO-1 and miR155 in *Tsc1*$^{GFAP-/-}$ mice precedes the development of seizures.

(A, B) Expression of 4-HNE in the hippocampus (HC) and cortex (Cx) of 2-week-old control mice was low while it was detectable in 2-week-old *Tsc1*$^{GFAP-/-}$ mice before seizure onset, however, only in the hippocampus mainly perivascular and in GFAP and occasionally NeuN expressing cells, but not Iba-1 positive cells **(B_1–B_3)**. **(C, D)** 4-HNE expression was higher in the hippocampus of 2-month-old control mice after seizure onset compared to 2-week old control mice before seizure onset. Two-month-old *Tsc1*$^{GFAP-/-}$ mice with recurrent seizures displayed high 4-HNE expression in the hippocampus and cortex with similar perivascular expression and co-localization with GFAP positive cells as in 2-week-old mice **(D_1–D_3)**. **(E, G)** HO-1 was moderately expressed in the hippocampus and cortex of 2-week-old and 2-month-old control mice. **(F)** In contrast, 2-week-old *Tsc1*$^{GFAP-/-}$ mice showed very high expression in sparsely distributed GFAP-positive cells mainly in the hippocampus before seizure onset (arrowheads, **F_1**). Iba-1 positive cells were in close

proximity to the HO-1 expressing cells, but did not show co-localization **($F_{2,3}$)**. **(H)** In 2-month-old *Tsc1*$^{GFAP-/-}$ mice with recurrent seizures the number of cells displaying strong HO-1 expression was higher than in animals before seizure onset and could also be found in the cortex. **(I–J)** Quantification of 4-HNE OD revealed higher 4-HNE reactivity in two-week-old animals in the HC and in HC and Cx in two-month-old mice. **(K)** Additionally, the count of cells with strong HO-1 expression increased in the HC and Cx in 2-month-old mice after seizure development **(F_1, H_1)**. **(L–O)** RNA quantification of miR155 and HO-1 in the hippocampus and cortex revealed higher expression in *Tsc1*$^{GFAP-/-}$ mice already before seizure onset compared to control, which was even higher in mice after the development of recurrent seizures. Scale bars: 500 μm (hippocampus) and 100 μm (cortex) in A, 50μm in B_1 (representative of B_1–B_3, D_1–D_3) and 20 μm in insert in F_1 (representative of F_1–F_3, H_1–H_3)). Mann-Whitney U-test. Data are expressed relative to expression observed in WT for the respective age group and presented as individual data points as well as in box plots. Error bars represent range; * $p<0.05$, ** $p<0.01$ (L–O $^{\#\#}$ $p<0.01$ 2-week-old vs. 2-month-old *Tsc1*$^{GFAP-/-}$ mice). n = 5 animals per group

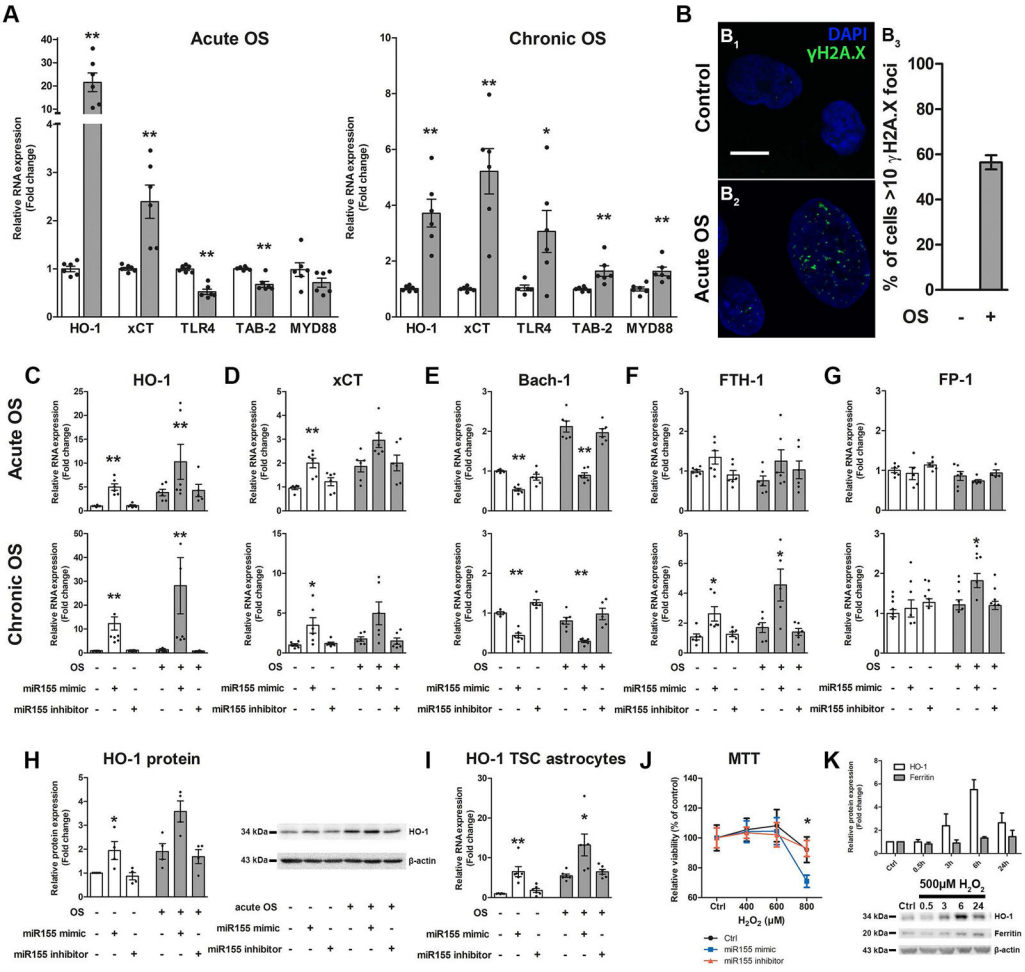

Fig. 4. *In vitro*, human fetal astrocytes displayed different response to acute vs. chronic OS and chronic HO-1 expression can induce genes involved in iron regulation.

(A) Acute OS rapidly induced gene expression of Nrf-2 targets HO-1 and xCT, while NF-κB signalling genes TLR-4 and TAB-2 were downregulated. Chronic OS increased expression of HO-1 and xCT. However, the HO-1 increase was lower than after acute OS. Moreover, in contrast to acute OS TLR-4, TAB-2 and MYD88 expression was increased. **(B)** Exposure to acute OS induced rapid expression of γH2A.X in the nucleus of human foetal astrocytes compared to control (B_2). Quantification of cells displaying >10 γH2A.X foci could not be detected in control cells, while acute OS induced expression in approx. 55% of cells (B_3). **(C, D, H, I)** Transfection of fetal astrocytes with miR155 mimic induced expression of HO-1 and xCT even in the absence of OS. This effect was preserved in cells derived from TSC patients and could be reversed by the inhibitor of miR155. **(E)** Additionally, Bach-1 expression was lower. These effects were independent of the presence of acute (3 h) or chronic (72 h) OS. **(F, G)** Transfection of fetal astrocytes with miR155 mimic for 24 h followed by acute OS had no effect on expression of FTH-1 and FPN-1. In contrast, prolonged exposure to the miR155 mimic for 72h coupled to chronic OS induced FTH-1 and FPN-1. **(J)** Moreover, fetal astrocytes exposed to miR155 mimic for 72 h displayed increased susceptibility to high H_2O_2 concentrations compared to control and miR155 inhibitor transfected cells as measured using the MTT assay. **(K)** Fetal astrocytes stimulated

with H_2O_2 for different time points displayed rapid expression of HO-1 protein which peaked at 6 h and decreased again after 24 h. In parallel, ferritin expression increased with a delay and remained high even after 24 h. Scale bar is 10 μm in B. Mann-Whitney U-test in A, J. Kruskal-Wallis test followed by Dunn's in C–I, K. Data are expressed relative to expression observed in control groups and the mean value as well as the individual data points are shown. Error bars represent SEM; *$p<0.05$, ** $p<0.01$, n = 3 independent cultures in duplicates (n = 379 cells (control) and 442 cells (acute OS) in B_3; 3 single cultures for H, I, K; 3 independent cultures in quadruplicates for J) per experiment

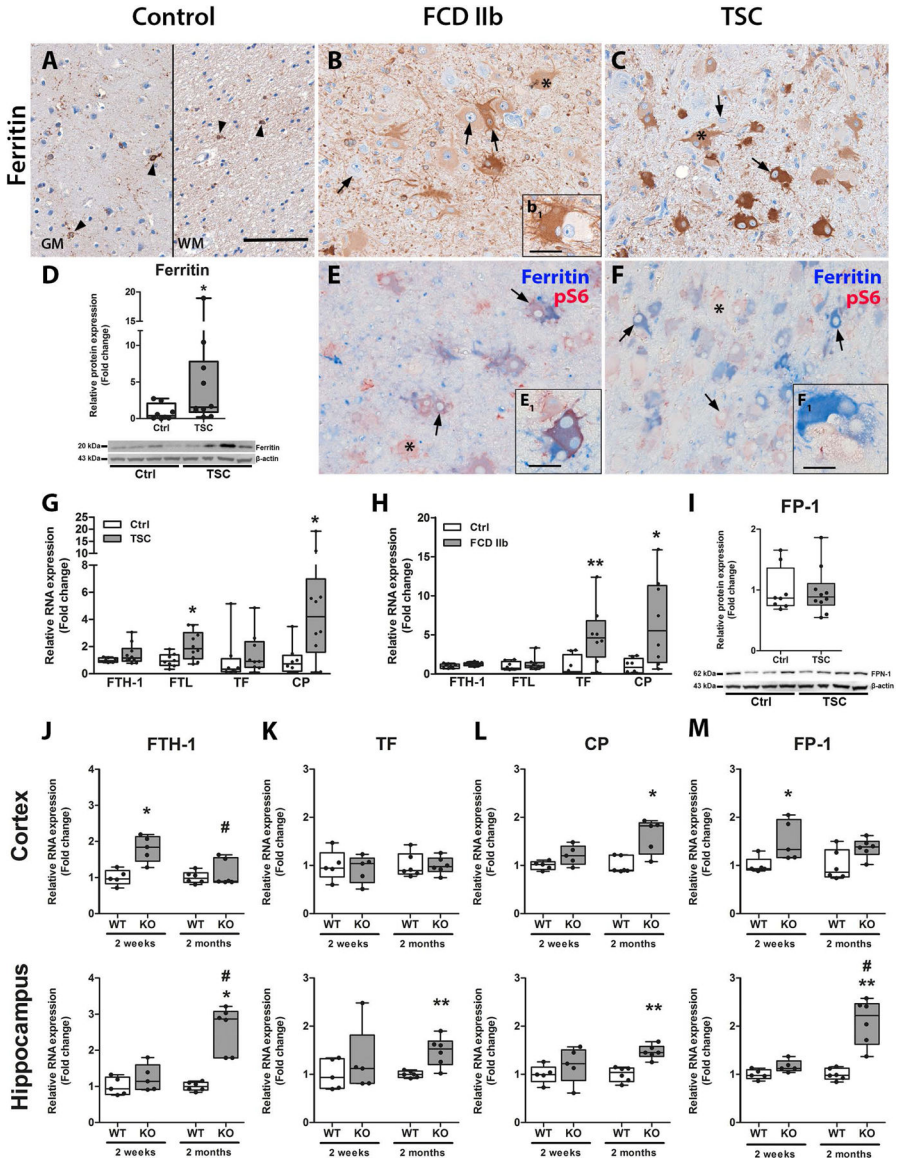

Fig. 5. Ferritin expression and other markers of iron homeostasis were altered in TSC, FCD IIb and in *Tsc1*$^{GFAP-/-}$ mice.

(A) Expression of ferritin in autoptic control tissue was restricted to cells with microglial morphology and very sporadically single cortical neurons (arrowheads). **(B, C)** In FCD IIb and TSC ferritin expression was high in the majority of dysmorphic neurons and balloon/giant cells. However, some cells displayed very weak ferritin expression (insert b_1). **(D)** Consistent with immunohistochemical evaluation, western blot analysis showed that total ferritin protein was higher in TSC patients as compared to control. **(E, F)** Double-labelling with pS6 revealed co-localization with the majority of pS6-positive cells in FCD IIb and TSC and additionally expression in cells with microglial morphology. Although most pS6 positive cells co-localized with ferritin some cells were negative for it (inserts E_1, F_1 red cells). **(G)** RNA expression revealed higher expression of FTL and CP in TSC tissue as compared to control. **(H)** In FCD IIb, expression of TF and CP was higher compared to controls. **(I)** The expression of the iron transporter FPN-1 was not different between FCD IIb

and TSC. **(J–M)** In the Cortex of *Tsc1*$^{GFAP-/-}$ mice expression of FTH1 and FP-1 was higher before seizure onset, while CP was higher after seizure development. In the hippocampus *Tsc1*$^{GFAP-/-}$ mice displayed higher FTH1, TF, CP and FP-1 expression after seizure onset. Scale bar 100 μm in A, 20 μm in inserts B_1, E_1, F_1. Mann-Whitney U-test. Data are expressed relative to expression observed in autopsy control tissue and control WT for the respective age group and presented as individual data points as well as in box plots. Error bars represent range; * $p<0.05$, ** $p<0.01$, *** $p<0.001$. n = 5 animals per group (J–M $^{\#}$ $p<0.05$ 2-week-old vs. 2-month-old *Tsc1*$^{GFAP-/-}$ mice). n = 8 (autopsy control, FCD IIb), n = 10 (TSC) (D, G–I)

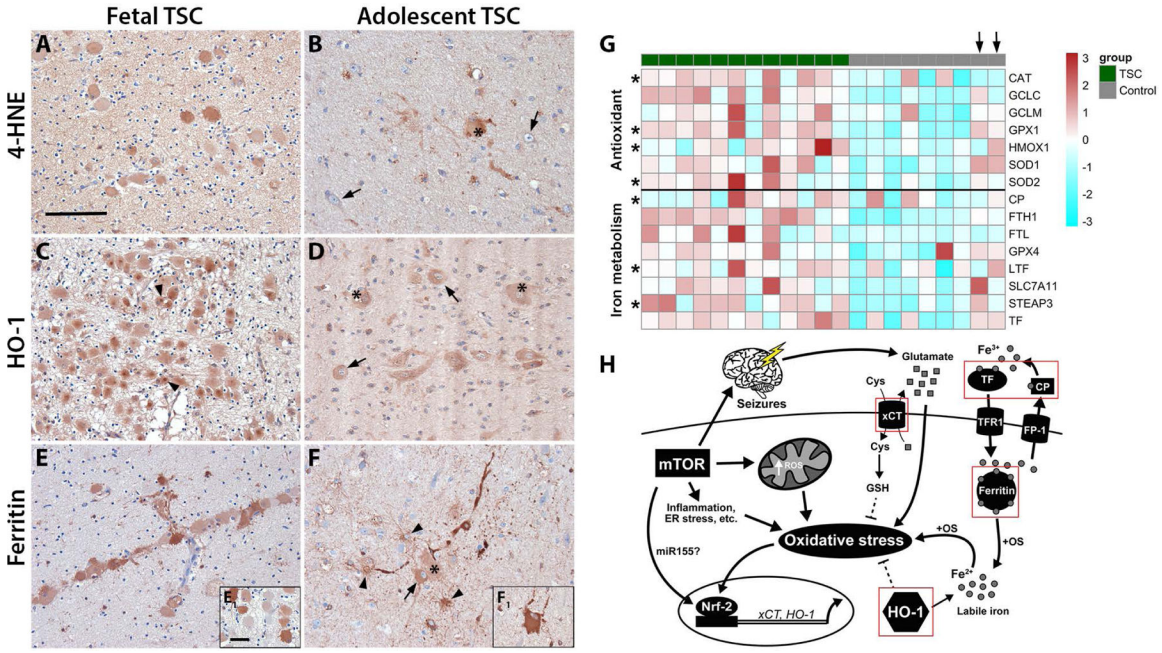

Fig. 6. Chronic activation of OS response genes and altered iron metabolism preceded birth and persisted until adulthood.

(A) Foetal TSC tissue displayed 4-HNE reactivity in many immature cells with giant cell morphology. **(B)** Surgically resected TSC tissue of older patients displayed sporadic 4-HNE reactivity predominantly in giant cells and cells with glial morphology but not dysmorphic neurons (arrows). **(C)** HO-1 expression in foetal TSC brain was high in the majority of giant cells (arrows) with frequent highly HO-1 reactive inclusions intracellularly next to the nucleus (arrowheads, insert in c). **(D)** In surgically resected TSC brain tissue of adolescent patients HO-1 expression was high in dysmorphic neurons and giant cells (arrows, asterisks). **(E)** Ferritin expression in foetal brain tissue was markedly high in many but not all giant cells (insert e_1). **(F)** In surgically resected brain tissue from older TSC patients cells displayed reactivity in dysmorphic neurons (arrows), giant cells (insert f_1, asterisks) and cells with astrocytic morphology (arrowheads). **(G)** Heat map showing enrichment of antioxidant genes and genes involved in iron metabolism in tubers from an independent cohort of TSC patients compared to autoptic control cortex. Please note the two control subjects indicated by an arrow on top that do show expression similar to the TSC cohort represent adult autopsy cases. Significant differences are indicated as asterisks in the respective row (Mann Whitney U test, BH-adjusted probabilities $p<0.05$). **(H)** Mechanisms of the interaction between mTOR activation and antioxidant gene expression in the context of OS. Chronic activation of mTOR increases metabolic demand and ER stress, as well as inflammation, all inducing production of excess ROS leading to expression of antioxidant genes, such as HO-1 and xCT. Acute activation has protective effects (dashed lines), while sustained activation in turn contributes to OS via e.g. elevated extracellular glutamate via xCT or excess free iron via HO-1. Disturbance in iron metabolism and seizures additionally contribute to free iron and glutamate and ultimately exacerbate OS even further. Components upregulated in TSC and FCD IIb are indicated by a red square. Sections A–C and J–L were counterstained with haematoxylin, Scale bar: 100 μm in A (representative for

A–F), 20 μm in E_1 (representative for inserts); arrows = dysmorphic neurons, arrowheads = inclusions in C, glia in F, asterisk = balloon/giant cells

Tab. 1

Immunoreactivity score (IRS) for 4-HNE, γH2A.X, Nrf-2 and HO-1 in surgically resected FCD IIb and TSC brain tissue.

	Control	FCD IIb	TSC
4-HNE	1 (1)	5 (4–6) *	4 (4)
γH2A.X	2 (1–4)	6 (4–9) *	6 (4–9) *
Nrf-2	3 (3–6)	6 (6–9) *	6 (3–9)
HO-1	2 (1–3)	2.5 (2–4)	3 (1–3)

The immunoreactivity score (IRS) is given as median with the range in brackets. Immunoreactivity was evaluated using a 0–3 scale (0 = absent, 1 = weak, 2 = moderate, 3 = strong staining). In addition, the number of positive cells was evaluated 0 = absent, 1 = rare, 2 = sparse, 3 = high). The product of these two scores (IRS) was calculated for each case. n = 5 (FCD IIb, TSC). Kruskal-Wallis test followed by the Dunn's post hoc test;

* $P < 0.05$ versus control.